

Hydrolysis of Uranium(VI) at Variable Temperatures (10–85 °C)

PierLuigi Zanonato,[†] Plinio Di Bernardo,[†] Arturo Bismondo,[‡] Guokui Liu,[§]
Xueyuan Chen,[§] and Linfeng Rao^{*||}

Contribution from the Dipartimento di Chimica Inorganica Metallorganica ed Analitica, Università di Padova, via Loredan 4, 35131, Padova, Italy; Istituto di Chimica Inorganica e delle Superfici del C.N.R. of Padova, Corso Stati Uniti 4, 35127, Padova, Italy; Chemistry Division, Argonne National Laboratory, Argonne, Illinois 60439; and Glenn T. Seaborg Center, Lawrence Berkeley National Laboratory, Berkeley, California 94720

Received November 30, 2003; E-mail: LRao@lbl.gov

Abstract: The hydrolysis of uranium(VI) in tetraethylammonium perchlorate (0.10 mol dm⁻³ at 25 °C) was studied at variable temperatures (10–85 °C). The hydrolysis constants ($^*\beta_{n,m}$) and enthalpy of hydrolysis ($\Delta H_{n,m}$) for the reaction $m\text{UO}_2^{2+} + n\text{H}_2\text{O} = (\text{UO}_2)_m(\text{OH})_n^{(2m-n)+} + n\text{H}^+$ were determined by titration potentiometry and calorimetry. The hydrolysis constants, $^*\beta_{1,1}$, $^*\beta_{2,2}$, and $^*\beta_{5,3}$, increased by 2–5 orders of magnitude as the temperature was increased from 10 to 85 °C. The enthalpies of hydrolysis, $\Delta H_{2,2}$ and $\Delta H_{5,3}$, also varied: $\Delta H_{2,2}$ became more endothermic while $\Delta H_{5,3}$ became less endothermic as the temperature was increased. The heat capacities of hydrolysis, $\Delta C_{p(2,2)}$ and $\Delta C_{p(5,3)}$, were calculated to be $(152 \pm 43) \text{ J K}^{-1} \text{ mol}^{-1}$ and $-(229 \pm 34) \text{ J K}^{-1} \text{ mol}^{-1}$, respectively. UV/Vis absorption spectra supported the trend that hydrolysis of U(VI) was enhanced at elevated temperatures. Time-resolved laser-induced fluorescence spectroscopy provided additional information on the hydrolyzed species at different temperatures. Approximation approaches to predict the effect of temperature were tested with the data from this study.

1. Introduction

Numerous studies have been conducted on the hydrolysis of uranium(VI) in aqueous solutions at or near 25 °C, but very few at elevated temperatures.^{1–3} In most of the studies, only the hydrolysis constants ($^*\beta_{n,m}$ for $m\text{UO}_2^{2+} + n\text{H}_2\text{O} = (\text{UO}_2)_m(\text{OH})_n^{(2m-n)+} + n\text{H}^+$) were obtained, where n and m range 1–5 and 1–9. Values of other thermodynamic parameters are either very scarce (e.g., the enthalpy of hydrolysis) or unknown (e.g., the heat capacity of hydrolysis). The scarcity of important thermodynamic parameters at 25 °C and the absence of data at elevated temperatures greatly limit the ability to predict the chemical behavior of uranium in the processing and disposal of nuclear wastes, where elevated temperatures are likely to be encountered.

The properties of water vary significantly as the temperature is changed. For example, the ionic product ($K_w = [\text{H}^+][\text{OH}^-]$) increases by almost 3 orders of magnitude⁴ and the dielectric constant decreases by approximately 35%⁵ from 0 to 100 °C. The increase in K_w is expected to have a great impact on the hydrolysis because the concentration of the hydroxide ion at the same concentration of the hydrogen ion becomes much higher at higher temperatures. On the other hand, the change in the dielectric constant is likely to perturb hydrolysis reactions because most hydrolyzed species are electrically charged and polynuclear. The degree of perturbation on different hydrolysis reactions could be different, which alters the speciation of U(VI) in solution. Therefore, the study of the hydrolysis of U(VI) at elevated temperatures can improve the fundamental understanding of these effects.

The equilibrium data for the hydrolysis reactions at any desired temperature can be predicted by using thermodynamic principles, provided that the enthalpy and entropy at the reference temperature (e.g., 25 °C) and their temperature dependencies are known. However, such data, especially the temperature dependencies, are rarely available in the literature. It is therefore necessary to rely on approximation approaches for prediction. The approaches that have been extensively discussed include the constant enthalpy approach,⁶ the constant

[†] Università di Padova.

[‡] Istituto di Chimica Inorganica e delle Superfici del C.N.R. of Padova.

[§] Argonne National Laboratory.

^{||} Lawrence Berkeley National Laboratory.

- (1) Grenthe, I.; Fuger, J.; Konings, R. J. M.; Lemire, R. J.; Muller, A. B.; Nguyen-Trung, C.; Wanner, H. *Chemical thermodynamics of uranium*; Wanner, H., Forest, I., Eds.; Elsevier Science Publishers B.V.: Amsterdam, 1992; pp 98–119.
- (2) Fuger, J.; Khodakovskiy, I. L.; Sergeeva, E. I.; Medvedev, V. A.; Navratil, J. D. *The Chemical Thermodynamics of Actinide Elements and Compounds: Part 12, The Actinide Aqueous Inorganic Complexes*; IAEA: Vienna, 1992; pp 31–41.
- (3) Guillaumont, R.; Fanghanel, T.; Fuger, J.; Grenthe, I.; Neck, V.; Palmer, D. A.; Rand, M. H. *Update on the chemical thermodynamics of uranium, neptunium, plutonium, americium and technetium*; Mompean, F. J., Illemassene, M., Domenech-Orti, C., Ben Said, K., Eds.; Elsevier B.V.: Amsterdam, 2003; pp 46–47, 64, 716, 724–728.

(4) Marshall, W. L.; Franck, E. U. *J. Phys. Chem. Ref. Data* **1981**, *10*, 295–304.

(5) Fernandez, D. P.; Goodwin, A. R. H.; Lemmon, E. W.; Sengers, J. M. H. L.; Williams, R. C. *J. Phys. Chem. Ref. Data* **1997**, *26* (4), 1125–1166.

heat capacity approach,⁶ the DQUANT equation,⁷ the Ryzhenko–Bryzgalin model,⁸ and the revised Helgeson–Kirkham–Flowers (HFK) equation.^{9–11} The applicability of the approximation methods needs to be tested with reliable experimental data in a wide range of temperature.

The objective of this study is to experimentally determine the equilibrium constants and the enthalpy of hydrolysis of U(VI) from 10 to 85 °C. Differing from most previous studies, the enthalpy of hydrolysis in this study has been directly determined at variable temperatures by calorimetry. Such data, for the first time, allow the calculation of the entropy of hydrolysis at variable temperatures and the heat capacity of hydrolysis from 10 to 85 °C. These important thermodynamic parameters provided valuable tools to evaluate the approximation methods. Additionally, spectroscopic data of optical absorption and time-resolved laser-induced fluorescence of U(VI) provided further information on the hydrolysis and the speciation of U(VI) in solution at variable temperatures.

2. Experimental Section

2.1. Chemicals. All chemicals were reagent grade or higher. Distilled/deionized water was used in preparations of all the solutions. Prior to use, the water was boiled and cooled in sealed bottles to reduce the amount of dissolved carbon dioxide. In this paper, all the concentrations in molarity are referred to 25 °C.

The stock solution of uranyl perchlorate was prepared by dissolving uranium trioxide (UO₃) in perchloric acid (Sigma–Aldrich, Inc., 70%). The concentration of uranium in the stock solution was determined by absorption spectrophotometry and fluorimetry.¹² Gran's titration method¹³ was used to determine the concentration of perchloric acid in the stock solutions. The titrant solution of tetraethylammonium hydroxide was prepared from a concentrated solution (Fluka, ~40%) and standardized against potassium hydrogen phthalate (Fluka, dried at 105 °C overnight). Precautions were taken to avoid the exposure of the stock solution of tetraethylammonium hydroxide to carbon dioxide in air. Gran's titrations indicated that the content of carbonate in the stock solution was less than 0.5%. Tetraethylammonium perchlorate (Fluka, 99%) was purified by recrystallization from water, washed with cold ethanol, and dried at 100–110 °C. The ionic strength of the working solutions was adjusted to 0.10 mol dm⁻³ at 25 °C by adding appropriate amounts of tetraethylammonium perchlorate as the background electrolyte.

2.2. Potentiometry. The potentiometric titrations were conducted at the University of Padova. The apparatus consisted of a 150 cm³ cell with a lid. Both the cell and the lid were water-jacketed and maintained at the desired temperatures by circulating water from a constant-temperature bath. It was important, especially for the titrations at temperatures above the ambient, to maintain the lid at the same temperature as the cell to avoid water condensation underneath the lid. Details of the titration setup have been provided elsewhere.¹⁴

The potentiometric titrations were performed in a pC_H (= -log[H⁺]) region from about 2.5 to 5.5. No precipitation of U(VI) was observed during the titration. Electromotive force (EMF, in millivolts) was

measured with an Amel pH meter (model 338) equipped with a Ross combination pH electrode (Orion model 8102). The electrode is workable up to 100 °C. The original electrode filling solution (3.0 mol dm⁻³ potassium chloride) was replaced with 1.0 mol dm⁻³ sodium perchlorate to avoid clogging of the electrode frit glass septum by the precipitation of KClO₄. The EMF in the acidic region can be expressed by eq 1.

$$E = E^\circ + RT/F \ln[H^+] + \gamma_H[H^+] \quad (1)$$

where R is the gas constant, F is the Faraday constant, and T is the temperature in kelvin. The last term is the electrode junction potential for the hydrogen ion ($\Delta E_{j,H^+}$), assumed to be proportional to the concentration of the hydrogen ion. Prior to each titration, an acid/base titration with standard perchloric acid and tetraethylammonium hydroxide was performed to obtain the electrode parameters of E° and γ_H . These parameters allowed the calculation of hydrogen ion concentrations from the EMF in the subsequent titration. Corrections for the electrode junction potential of the hydroxide ion were not necessary in these experiments.

Detailed experimental conditions of potentiometry are shown in Table S1 of the Supporting Information. Standardized tetraethylammonium hydroxide was added into an acidic U(VI) solution ($V^\circ = 20\text{--}130\text{ cm}^3$). The EMF data were collected at time intervals determined by the data collection criterion; that is, the drift of EMF (ΔE) was less than 0.1 mV for 180 s. Fifty to seventy data points were collected in each titration. Multiple titrations were conducted at each temperature with solutions of different concentrations ($C_{H^+} = 2\text{--}36\text{ mmol dm}^{-3}$ and $C_{U^\circ} = 0.4\text{--}11\text{ mmol dm}^{-3}$). The hydrolysis constants of U(VI) on the molarity scale were calculated with the program Hyperquad.¹⁵ To allow the comparison at different temperatures, the constants in molarity should usually be converted to the constants in molality by using the density of the solution, as suggested by Grenthe et al.¹⁶ However, such conversion is unnecessary for the system in this study, since the density of 0.10 mol dm⁻³ tetraethylammonium perchlorate at 25 °C is 1.0005 g cm⁻³. The difference between the values in molarity and molality for this system is negligible.

2.3. Calorimetry. The calorimetric titrations were conducted with both an isothermal microcalorimeter (model ITC 4200, Calorimetry Sciences Corp.) at the Lawrence Berkeley National Laboratory (for t from 25 to 85 °C) and an isoperibol calorimeter (model 87-558, Tronac) at the University of Padova (for t from 10 to 40 °C). The microcalorimeter is operable up to 85 °C but not suitable at 10 °C due to the lack of a dry nitrogen purging system that was necessary to prevent condensation inside the calorimeter. The isoperibol calorimeter is suitable for lower temperatures (up to 40 °C). As a result, the titrations above 40 °C were exclusively conducted with the microcalorimeter at Berkeley, while the titrations at 10 °C were exclusively conducted at Padova. The titrations at 25 and 40 °C were conducted at both laboratories so that the results could be compared and the internal consistency of the data in the whole range of temperature (from 10 to 85 °C) was tested. Detailed experimental conditions of calorimetry are shown in Table S2 of the Supporting Information. The highest pC_H in all the titrations was 5.5 to avoid precipitation of hydrolyzed U(VI) species.

The microcalorimeter uses a “twin” heat flow design to reach the maximum sensitivity. The reaction heat is measured from the difference in the heat flows between the sample and the reference cells. The volume of the cells is about 1.2 cm³. The titrant is delivered into the sample cell through a long and thin needle from a 100 μL or 250 μL syringe. The syringe is driven by a precision stepper motor that guarantees accurate delivery of the titrant. The performance of the

(6) Puigdomenech, I.; Plyasunov, A. V.; Rard, J. A.; Grenthe, I. In *Modeling in Aquatic Chemistry*; Grenthe, I., Puigdomenech, I., Eds.; Temperature corrections to thermodynamic data and enthalpy calculations; NEA/OECD: Paris, 1997; Chapter X.

(7) Helgeson, H. C. *J. Phys. Chem.* **1967**, *71*, 3121–3136.

(8) Ryzhenko, B. N.; Bryzgalin, O. V.; Shapkin, A. I. *Geochem. Int.* **1991**, *28* (5), 77–83.

(9) Shock, E. L.; Helgeson, H. C. *Geochim. Cosmochim. Acta* **1988**, *52*, 2009–2036.

(10) Tanger, IV, J. C.; Helgeson, H. C. *Am. J. Sci.* **1988**, *288*, 19–98.

(11) Shock, E. L.; Sassani, D. C.; Betz, H. *Geochim. Cosmochim. Acta* **1997**, *61*, 4245–4266.

(12) Sill, C. W.; Peterson, H. E. *Anal. Chem.* **1947**, *19*, 646–651.

(13) Gran, G. *Analyst* **1952**, *77*, 661.

(14) Zanonato, P.; Di Bernardo, P.; Bismondo, A.; Rao, L.; Choppin, G. R. *J. Solution Chem.* **2001**, *30*, 1–18.

(15) Gans, P.; Sabatini, A.; Vacca, A. *Talanta* **1996**, *43*, 1739–1753.

(16) Grenthe, I.; Puigdomenech, I. In *Modeling in Aquatic Chemistry*; Grenthe, I., Puigdomenech, I., Eds.; *Symbols, Standards, and Conventions*; NEA/OECD: Paris, 1997; Chapter II.

calorimeter has been tested by measuring the enthalpy of protonation of tris(hydroxymethyl)aminomethane (THAM). The results (in kJ mol⁻¹) are -47.7 ± 0.3 (25 °C), -46.8 ± 0.2 (40 °C), -45.8 ± 0.5 (55 °C), -45.2 ± 0.5 (70 °C), and -43.1 ± 0.8 (85 °C), which compared well with the values in the literature: -46.0 ± 0.3 at 45 °C and -46.2 ± 0.3 at 70 °C,¹⁷ -46.81 ± 0.02 at 35 °C, and -46.0 ± 0.02 at 50 °C.¹⁸ In the titrations of U(VI) hydrolysis, the initial cell solutions (~ 0.90 cm³ at 25 °C) usually contained $0.2\text{--}1.6$ mmol dm⁻³ UO₂(ClO₄)₂ and $0.6\text{--}3.0$ mmol dm⁻³ HClO₄. The titrant (~ 20 mmol dm⁻³ tetraethylammonium hydroxide) was added in small increments ($2\text{--}5$ μL). After the titration was completed, the pH was measured and the solution was examined by laser light scattering to be certain that no precipitation of U(VI) occurred.

The descriptions of the isoperibol calorimeter were given elsewhere.¹⁹ Two types of titrations were performed: (1) a forward titration where a 20 cm³ acidic solution of U(VI) was titrated with 0.1 mol dm⁻³ tetraethylammonium hydroxide and (2) a backward titration where a 20 cm³ solution of U(VI) (partially hydrolyzed) was titrated with 0.1 mol dm⁻³ perchloric acid.

Multiple titrations with different concentrations of UO₂(ClO₄)₂ and HClO₄ were conducted at each temperature. For each titration, n additions were made (usually $n = 50\text{--}70$), resulting in n experimental values of the total heat generated in the reaction cell ($Q_{\text{ex},j}$, $j = 1$ to n). These values were corrected for the heat of dilution of the titrant ($Q_{\text{dil},j}$), which was determined in separate runs. The net reaction heat at the j -th point ($Q_{\text{r},j}$) was obtained from the difference: $Q_{\text{r},j} = Q_{\text{ex},j} - Q_{\text{dil},j}$. Two quantities, $\Delta h_{\text{v,M}}$ and $\Delta h_{\text{v,OH}}$, were then calculated by

$$\Delta h_{\text{v,M}} = (Q_{\text{r},j} - Q_{\text{p},j})/n_{\text{M}} \quad (2)$$

$$\Delta h_{\text{v,OH}} = (Q_{\text{r},j} - Q_{\text{r},j-1})/n_{\text{j,OH}} \quad (3)$$

where $Q_{\text{p},j}$ was the heat due to the formation of water at the j -th point and n_{M} was the number of moles of U(VI) in the cell and $n_{\text{j,OH}}$ was the number of moles of hydroxide added at the j -th addition. The enthalpy of hydrolysis was calculated by the computer program Letagrop,²⁰ modified in this work to use $\Delta h_{\text{v,M}}$ as the error-carrying variable while assigning equal weight to all the titrations with different amounts of U(VI).

Separate calorimetric titrations were conducted to determine the enthalpy of water formation in 0.10 mol dm⁻³ tetraethylammonium perchlorate at variable temperatures. These values were needed in the calculation of the enthalpy of hydrolysis of U(VI).

2.4. UV/Vis Absorption Spectroscopy. UV/Vis absorption spectra of four U(VI) solutions (A–D) were collected at 10 and 85 °C on a Varian Cary-5G spectrometer equipped with a 1 × 1 Peltier automatic temperature controller (± 0.1 °C). Quartz cells (10 mm) were used. The concentrations of free acid and U(VI) (C_{H} and C_{U} in mmol dm⁻³) in the solutions are (A) 0.1/0.1, (B) $-0.05/0.1$, (C) $-0.14/0.1$, and (D) “0”/0.01, where $-C_{\text{H}} = C_{\text{OH}}$ and solution D was neutral.

2.5. Time-Resolved Laser-Induced Fluorescence Spectroscopy. The fluorescence emission spectra and lifetime of the U(VI) solutions (A–D) at 20, 40, 60, and 80 °C were studied at Argonne National Laboratory. The fluorescence was induced by a tunable pulsed dye laser pumping the charge-transfer transition of U(VI) species. The laser provided 5-ns pulses with a repetition rate of 10 Hz. The pumping laser was tuned between 423 and 425 nm where the U(VI) species in solution showed maximum absorption. The fluorescence decay was measured on the selected emission at 515 nm. Each decay curve was averaged over 800 pulses using a digital storage oscilloscope.

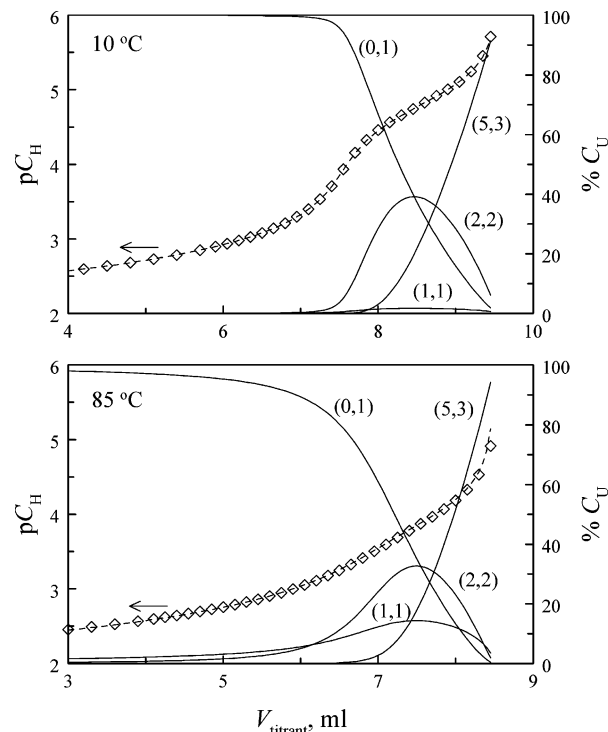
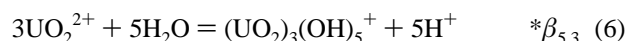


Figure 1. Potentiometric titration of U(VI) hydrolysis, $I = 0.10$ mol dm⁻³ (C₂H₅)₄NClO₄. Titrant concentration ((C₂H₅)₄NOH) in mmol dm⁻³: 98.1 (10 °C), 102.0 (85 °C). Initial cup solution (V°) in mL: 130.0 (10 °C), 110.1 (85 °C). Initial cup concentrations ($C_{\text{H}}/C_{\text{U}}$, mmol dm⁻³): 5.83/0.855 (10 °C), 6.47/0.863 (85 °C). Symbols: (◇) experimental data (pC_{H}); (dashed curve) fit (pC_{H}); (solid lines) percentage of U(VI) species (right y-axis).

3. Results

3.1. Hydrolysis Constants. The data of 25 potentiometric titrations at 10–85 °C are provided in Table S3 of the Supporting Information. Two representative titrations are shown in Figure 1. In the region of pC_{H} from 2.5 to 5.5, the best fit was obtained by including three hydrolysis species in the calculation, i.e., the (1,1), (2,2), and (5,3) species defined by the following reactions:



This agreed with a previous study at 25 and 94 °C where the same species were observed before precipitation of U(VI) occurred.²¹ The hydrolysis constants at different temperatures are listed in Table 1. The values of $\log * \beta_{1,1}$ have larger uncertainties because the concentration of the (1,1) species was usually low. The data indicate that the hydrolysis constants increased by about 2 orders ($* \beta_{1,1}$ and $* \beta_{2,2}$) or 5 orders ($* \beta_{5,3}$) of magnitude, as the temperature was increased from 10 to 85 °C.

3.2. Enthalpy of Hydrolysis. The results of calorimetry at 40 °C were shown in Figure 2 in the form of $\Delta h_{\text{v,M}}$ vs \bar{n}_{OH} . The value \bar{n}_{OH} is the average number of hydroxide on each U(VI) and was calculated using the hydrolysis constants in Table 1 and the concentrations of U(VI) and OH⁻. The enthalpy of

(17) Smith, R.; Zanonato, P.; Chopin, G. R. *J. Chem. Thermodyn.* **1992**, *24*, 99–106.

(18) Grenthe, I.; Ots, H.; Ginstrup, O. *Acta Chem. Scand.* **1970**, *24*, 1067.

(19) Cassol, A.; Di Bernardo, P.; Portanova, R.; Tolazzi, M.; Tomat, G.; Zanonato, P. *Inorg. Chem.* **1990**, *29*, 1079–1084.

(20) Arnek, R. *Ark. Kemi* **1970**, *32*, 81.

(21) Baes, C. F., Jr.; Meyer, N. J. *Inorg. Chem.* **1962**, *1* (4), 780–789.

Table 1. Equilibrium Constants and Thermodynamic Parameters for U(VI) Hydrolysis, $m\text{UO}_2^{2+} + n\text{H}_2\text{O} = (\text{UO}_2)_m(\text{OH})_n^{(2m-n)+} + n\text{H}^+$ ($I = 0.10 \text{ mol dm}^{-3}$ ($\text{C}_2\text{H}_5)_4\text{NClO}_4$. The Error Limits = 3σ)

reaction	T_i , °C	$\log^* \beta_{n,m}$ or $\text{p}K_w$	$\log^* \beta_{n,m}^{\circ}$ ^a	$\Delta G_{n,m}^{\circ}$ kJ mol ⁻¹	$\Delta H_{n,m}$ or ΔH_w kJ mol ⁻¹	$\Delta S_{n,m}$ J K ⁻¹ mol ⁻¹
$m = 1, n = 1$	10	-6.1 ± 0.3	-5.9 ± 0.3	32.1		
$\text{UO}_2^{2+} + \text{H}_2\text{O} =$	25	-5.58 ± 0.24	-5.40 ± 0.24^b	30.8	46.5 ± 3.7^c	53 ± 13^c
$\text{UO}_2\text{OH}^+ + \text{H}^+$	40	-5.11 ± 0.11	-4.92 ± 0.12	29.5		
	55	-5.07 ± 0.24	-4.88 ± 0.24	30.6		
	70	-4.51 ± 0.11	-4.31 ± 0.12	28.3		
	85	-4.24 ± 0.15	-4.03 ± 0.15	27.6	58 ± 7	85 ± 30
$m = 2, n = 2$	10	-6.30 ± 0.02	-6.09 ± 0.04	33.0	51.5 ± 0.9	65.3 ± 3.6
$2\text{UO}_2^{2+} + 2\text{H}_2\text{O} =$	25	-5.83 ± 0.02	-5.62 ± 0.04^d	32.1	48.2 ± 1.7	54 ± 6
$(\text{UO}_2)_2(\text{OH})_2^{2+} + 2\text{H}^+$	40	-5.43 ± 0.01	-5.21 ± 0.03	31.2	50 ± 2	60 ± 6
	55	-5.06 ± 0.03	-4.84 ± 0.05	30.4	53 ± 8	69 ± 24
	70	-4.73 ± 0.03	-4.50 ± 0.05	29.6	58 ± 3	83 ± 7
	85	-4.49 ± 0.03	-4.25 ± 0.05	29.1	61 ± 2	89 ± 6
$m = 3, n = 5$	10	-17.52 ± 0.01	-16.90 ± 0.04	91.61	128.0 ± 0.5	128.5 ± 2.0
$3\text{UO}_2^{2+} + 5\text{H}_2\text{O} =$	25	-16.37 ± 0.02	-15.74 ± 0.05^e	89.84	120.1 ± 1.6	101.5 ± 5.7
$(\text{UO}_2)_3(\text{OH})_5^+ + 5\text{H}^+$	40	-15.35 ± 0.01	-14.70 ± 0.04	88.12	119 ± 2	99 ± 6
	55	-14.45 ± 0.02	-13.78 ± 0.05	86.57	113 ± 7	80 ± 21
	70	-13.61 ± 0.02	-12.92 ± 0.05	84.87	112 ± 3	79 ± 9
	85	-12.94 ± 0.02	-12.22 ± 0.05	83.78	110 ± 2	73 ± 6
$\text{H}^+ + \text{OH}^- = \text{H}_2\text{O}$	10	14.37 ± 0.01			-60.8 ± 0.1	
	25	13.78 ± 0.01			-56.7 ± 0.5	
	40	13.39 ± 0.01			-52.9 ± 0.5	
	55	12.99 ± 0.01			-50.8 ± 0.8	
	70	12.65 ± 0.02			-48.6 ± 1.2	
	85	12.36 ± 0.03			-45.3 ± 1.5	

^a Calculated by the specific ion interaction theory (SIT), discussions provided in section 4.1. ^b $\log^* \beta_{1,1}^{\circ}$ at 25 °C from the literature: -5.25 ± 0.24 (ref 3), -5.19 ± 0.05 (ref 22), -5.1 ± 0.1 (ref 23). ^c Calculated from the linear fit of $\log \beta_{1,1}$ vs $1/T$. ^d $\log^* \beta_{2,2}^{\circ}$ at 25 °C from the literature: -5.62 ± 0.04 (ref 3), -5.76 ± 0.04 (ref 22, 24), -5.56 ± 0.06 (ref 23). ^e $\log^* \beta_{3,3}^{\circ}$ at 25 °C from the literature: -15.55 ± 0.12 (ref 3), -15.89 ± 0.06 (ref 22, 24), -15.46 ± 0.09 (ref 23).

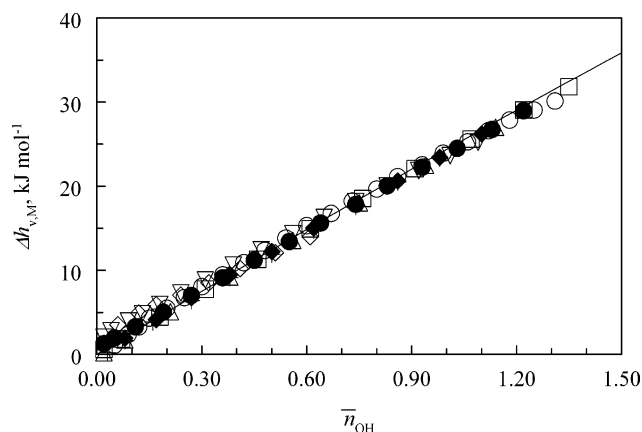


Figure 2. Plot of $\Delta h_{v,M}$ vs \bar{n}_{OH} for the calorimetric titrations of U(VI) hydrolysis at 40 °C, $I = 0.10 \text{ mol dm}^{-3}$ ($\text{C}_2\text{H}_5)_4\text{NClO}_4$. (Symbols) experimental data of eight titrations (The number of data points is reduced for clarity. Detailed conditions are in Table S2 of the Supporting Information); (line) calculated with the constants and enthalpy of hydrolysis in Table 1.

hydrolysis of U(VI) was calculated and listed in Table 1. Because the (1,1) species was insignificant at lower temperatures, the uncertainties of $\Delta H_{1,1}$ were usually quite high and its inclusion in the calculation did not improve the overall goodness of the fit. As a result, the value of $\Delta H_{1,1}$ was obtained only at 85 °C. In Figure 2, the calculated line agrees very well with the experimental data of eight titrations, reflecting the mutual consistency of the calorimetric and potentiometric data on the hydrolysis of U(VI). Typical raw data of the calorimetric titrations are presented in Figure S1 of the Supporting Information, with a titration thermogram from the microcalorimeter and a plot of $\Delta h_{v,\text{OH}}$ vs $C_{\text{H}}/C_{\text{U}}$.

3.3. UV/Vis Absorption Spectra. The UV/Vis absorption spectra of the four U(VI) solutions at 10 and 85 °C are shown in Figure 3. A few trends are shown by the spectra: (1) at each

temperature, the maxima of the spectra were shifted to longer wavelengths and the absorbance became significantly higher from A to B and to C as the acidity decreased; (2) for solutions A, B, and D, the maximum of the spectrum was shifted to a longer wavelength and the absorbance was higher as the temperature was increased from 10 to 85 °C; (3) for solution C, though it is difficult to accurately identify the wavelength of maximum absorption due to the split feature of the peak, it is evident that the absorption increased when the temperature was increased from 10 to 85 °C.

3.4. Fluorescence. The fluorescence emission spectra and lifetime of solutions B and C were obtained at 20, 40, 60, and 80 °C. When the temperature was increased, the fluorescence lifetime of each solution decreased, whereas little change was observed in the patterns of the emission spectra (Figure S2 of the Supporting Information). The decay of the fluorescence of U(VI) in both solutions was shown in Figure S3 of the Supporting Information and fitted with a single-exponential function of time. However, it appears that, after the fluorescence intensity decreased by more than 2 orders of magnitude, the decay curves for both solutions start to deviate from the single-exponential behavior. This may suggest the existence of minor uranyl species with a longer lifetime in the solutions. Therefore, attempts were made to fit the fluorescence decay with two exponential functions. It was found that, while the lifetime for the first component did not change noticeably from that of the single-exponential fit, the result for the second component was poor with very high uncertainty. We cannot rule out the presence of other uranyl species with longer lifetime in these solutions, but the percentage of such species is so low that reliable calculations of the lifetime cannot be made. After all, the calculated lifetime for the dominant component is not altered whether the minor component is included. As a result, the lifetimes calculated by the single-exponential decay are accepted

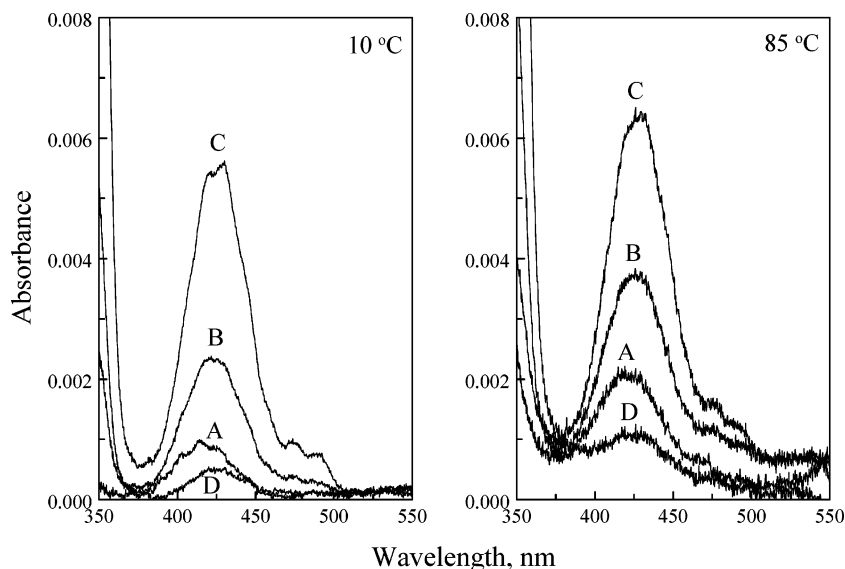


Figure 3. UV/Vis absorption spectra of U(VI) solutions at 10 and 85 °C, optical path = 1.00 cm, $I = 0.10 \text{ mol dm}^{-3}$ $(\text{C}_2\text{H}_5)_4\text{NClO}_4$. The approximate wavelengths ($\pm 1 \text{ nm}$) for maximum absorbance at 10 and 85 °C: (A) 414, 419; (B) 425, 426; (C) ~ 430 , ~ 430 ; (D) 423, 426. $C_{\text{H}}/C_{\text{U}}$ (mmol dm^{-3}): (A) 0.1/0.1, (B) $-0.05/0.1$, (C) $-0.14/0.1$, (D) neutral/0.01.

Table 2. Fluorescence Lifetime for the U(VI) Solutions at Different Temperatures

solution ^a	$T, ^\circ\text{C}$	speciation (%) ^b				lifetime $\tau, \mu\text{s}$	activation parameter	
		(0,1)	(1,1)	(2,2)	(5,3)		E_a kJ mol^{-1}	A
B	20	48.1	6.5	28.8	16.6	19.5	34.8 ± 3.4	7.6×10^{10}
	40	41.7	10.1	28.1	20.1	9.14		
	60	34.0	16.8	25.0	24.2	3.12		
	80	25.4	28.2	20.1	26.3	2.09		
C	20	7.6	4.2	12.1	76.1	25.8	37.2 ± 3.7	1.4×10^{11}
	40	6.2	6.2	10.4	77.2	13.0		
	60	4.5	9.4	8.0	78.1	4.05		
	80	2.8	14.4	5.2	77.6	2.40		

^a Concentrations ($C_{\text{OH}}/C_{\text{U}}$ in mmol dm^{-3}): 0.05/0.1 (solution B); 0.14/0.1 (solution C). ^b Species: (0,1) UO_2^{2+} , (1,1) $\text{UO}_2(\text{OH})^+$, (2,2) $(\text{UO}_2)_2(\text{OH})_2^{2+}$, (5,3) $(\text{UO}_2)_3(\text{OH})_5^+$. ^c Values for (5,3) species in the literature: τ at 20 °C (μs) 25.3 ($I = 0.5 \text{ mol dm}^{-3}$),²⁵ 35.7 ($I = 0.5 \text{ mol dm}^{-3}$),²⁶ 23.0 ($I = 0.1 \text{ mol dm}^{-3}$);²⁷ E_a (kJ mol^{-1}) 22.9 ($I = 0.5 \text{ mol dm}^{-3}$),²⁷ 37.6 ($I = 0.5 \text{ mol dm}^{-3}$).²⁶

and shown in Table 2, together with the speciation of U(VI) calculated with the hydrolysis constants in Table 1.

The temperature dependence of the fluorescence lifetime obeys the Arrhenius law (Figure S4 of the Supporting Information), consistent with previous studies on similar hydroxo complexes.^{25,26} The activation parameters obtained from the Arrhenius plot are also shown in Table 2. The fluorescence of solutions A and D was too weak to allow reliable analysis.

4. Discussion

4.1. Calculation of the Thermodynamic Parameters to Standard State Conditions. As preferred in common compilations of thermodynamic data, the standard state is defined as the infinite dilute solution, with pure water as the solvent. The SIT (Specific Ion Interaction Theory) method originated from

the Brønsted–Guggenheim–Scatchard model^{28–30} has been used to calculate the hydrolysis constants at zero ionic strength. For reactions 4, 5, and 6, the hydrolysis constants at the standard state ($\log {}^*\beta_{n,m}^\circ$) are calculated by the following equations:

$$\log {}^*\beta_{1,1} + 2D = \log {}^*\beta_{1,1}^\circ - \Delta\epsilon_{1,1}I_m \quad (7)$$

$$\log {}^*\beta_{2,2} + 2D = \log {}^*\beta_{2,2}^\circ - \Delta\epsilon_{2,2}I_m \quad (8)$$

$$\log {}^*\beta_{5,3} + 6D = \log {}^*\beta_{5,3}^\circ - \Delta\epsilon_{5,3}I_m \quad (9)$$

where $D = AI_m^{1/2}/(1 + 1.5AI_m^{1/2})$, the Debye–Huckel term used in the SIT method, and I_m is the ionic strength in molality. $\Delta\epsilon_{1,1} = \epsilon(\text{UO}_2\text{OH}^+, \text{ClO}_4^-) + \epsilon(\text{H}^+, \text{ClO}_4^-) - \epsilon(\text{UO}_2^{2+}, \text{ClO}_4^-)$, $\Delta\epsilon_{2,2} = \epsilon((\text{UO}_2)_2(\text{OH})_2^{2+}, \text{ClO}_4^-) + 2\epsilon(\text{H}^+, \text{ClO}_4^-) - 2\epsilon(\text{UO}_2^{2+}, \text{ClO}_4^-)$, and $\Delta\epsilon_{5,3} = \epsilon((\text{UO}_2)_3(\text{OH})_5^+, \text{ClO}_4^-) + 5\epsilon(\text{H}^+, \text{ClO}_4^-) - 3\epsilon(\text{UO}_2^{2+}, \text{ClO}_4^-)$. The specific ion interaction parameters (kg mol^{-1}) at 25 °C are the following: $\epsilon(\text{H}^+, \text{ClO}_4^-) = 0.14 \pm 0.02$, $\epsilon(\text{UO}_2^{2+}, \text{ClO}_4^-) = 0.46 \pm 0.03$, $\epsilon(\text{UO}_2\text{OH}^+, \text{ClO}_4^-) = -0.06 \pm 0.40$, $\epsilon((\text{UO}_2)_2(\text{OH})_2^{2+}, \text{ClO}_4^-) = 0.57 \pm 0.07$, $\epsilon((\text{UO}_2)_3(\text{OH})_5^+, \text{ClO}_4^-) = 0.45 \pm 0.15$.³ For the calculation of $\log {}^*\beta_{n,m}^\circ$ at temperatures other than 25 °C, the Debye–Huckel term was calculated with the values of A at different temperatures³¹ and the ion interaction parameters at 25 °C were used because the values at other temperatures were not known. Using the interaction parameters at 25 °C may introduce some errors into the $\log {}^*\beta_{n,m}^\circ$. However, the errors are probably quite small, since the ionic strength in this study is low and the values of $(\partial\epsilon/\partial T)_p$ are usually $\leq 0.005 \text{ kg mol}^{-1} \text{ K}^{-1}$ for temperatures below 200 °C.³ Besides, the values of $(\partial\epsilon/\partial T)_p$ for the reactants and products may balance out each other so that $\Delta\epsilon$ for many reactions remains approximately constant up to 100 °C.³² The

(22) De Stefano, C.; Gianguzza, A.; Leggio, T.; Sammartano, S. *J. Chem. Eng. Data* **2002**, *47*, 533–538.

(23) Brown, P. L. *Radiochim. Acta* **2002**, *90*, 589–593.

(24) Gianguzza, A.; Milea D.; Millero, F. J.; Sammartano, S. *Mar. Chem.* **2004**, *85*, 103–124.

(25) Eliet, V.; Grenthe, I.; Bidoglio, G. *Appl. Spectrosc.* **2000**, *54*, 99–105.

(26) Kimura, T.; Nagaiishi, R.; Ozaki, T.; Arisaka, M.; Yoshida, Z. *J. Nucl. Sci. Technol.* **2002**, Supplement 3, 233–239.

(27) Moulin, C.; Laszak, I.; Moulin, V.; Tondre, C. *Appl. Spectrosc.* **1998**, *52*, 528.

(28) (a) Brønsted, J. N. *J. Am. Chem. Soc.* **1922**, *44*, 877–898. (b) Brønsted, J. N. *J. Am. Chem. Soc.* **1922**, *44*, 938–948.

(29) Guggenheim, E. A. *Philos. Mag.* **1935**, *57* (seventh series), 588–643.

(30) Scatchard, G. *Chem. Rev.* **1936**, *19*, 309–327.

(31) Helgeson, H. C.; Kirkham, D. H.; Flowers, G. C. *Am. J. Sci.* **1981**, 1249–1516.

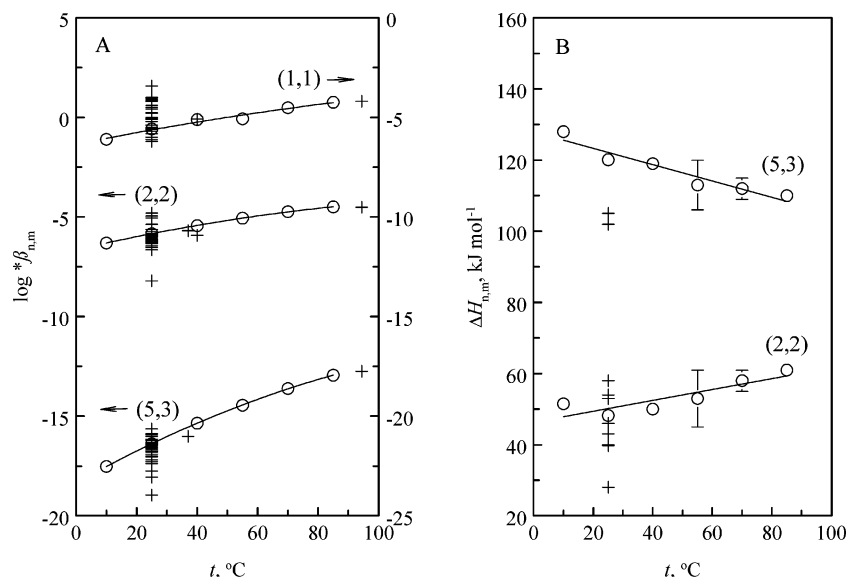


Figure 4. Hydrolysis constants (A) and enthalpy of hydrolysis (B) of U(VI) at variable temperatures. Symbols: (○) Data from this work, $I = 0.10 \text{ mol dm}^{-3}$ $(\text{C}_2\text{H}_5)_4\text{NClO}_4$, (+) data from the literature,¹ $I = 0.1\text{--}7.5 \text{ mol dm}^{-3}$.

calculated $\log * \beta_{n,m}^{\circ}$ and $\Delta G_{n,m}^{\circ}$ at different temperatures are listed in Table 1.

Correction of the enthalpy data to the standard state requires the knowledge of $(\partial\epsilon/\partial T)_p$ as well as the partial molar enthalpy of water at the specific ionic strength and temperature.³³ However, since the $\Delta\epsilon$ for many reactions remains approximately constant up to $100 \text{ }^{\circ}\text{C}$ (usually on the order of $10^{-3} \text{ kg mol}^{-1}$), a rough estimate of the correction ($\Delta H_{n,m}^{\circ} - \Delta H_{n,m}$) is $\leq 0.5 \text{ kJ mol}^{-1}$ at $I_m = 0.1 \text{ mol kg}^{-1}$, smaller than the uncertainties of the experimental $\Delta H_{n,m}$. As a result, no corrections for ionic strength were performed on the enthalpy of hydrolysis from this study.

From the entropy of hydrolysis in Table 1, the standard molar entropies of UO_2OH^+ , $(\text{UO}_2)_2(\text{OH})_2^{2+}$, and $(\text{UO}_2)_3(\text{OH})_5^+$ at $25 \text{ }^{\circ}\text{C}$ were calculated to be 24 ± 13 , -2 ± 12 , and 157 ± 15 , compared with the estimated values of 17 ± 50 , -38 ± 15 , and $83 \pm 30 \text{ J K}^{-1} \text{ mol}^{-1}$ for the same species in the literature.

4.2. Effect of Temperature on the Hydrolysis Constants and Enthalpy. In Figure 4A, the hydrolysis constants from this work are plotted as a function of temperature. Data from the literature, approximately 30, 50, and 40 values of $\log * \beta_{1,1}$, $\log * \beta_{2,2}$, and $\log * \beta_{5,3}$ at $25 \text{ }^{\circ}\text{C}$ ($I = 0\text{--}7.5 \text{ mol dm}^{-3}$) and a few values at other temperatures,^{1–3} are also shown for comparison.

All three hydrolysis constants increase as the temperature is increased but to different extents. Consequently, the speciation of U(VI) at elevated temperatures differs from that at lower temperatures as shown in Figure 5, where two major trends can be observed: (1) the percentage of free $\text{UO}_2^{2+}(\text{aq})$ is much lower at $85 \text{ }^{\circ}\text{C}$ than that at $10 \text{ }^{\circ}\text{C}$, indicating the enhancement of overall hydrolysis at elevated temperatures; (2) the (1,1) species, UO_2OH^+ , becomes more important at higher temperatures and lower concentrations of U(VI). The enhancement of hydrolysis at elevated temperatures is mainly due to the increase of the degree of ionization of water that results in an increase of 2 orders of magnitude in the concentration of the hydroxide ion (at the same

pC_{H}) from 10 to $85 \text{ }^{\circ}\text{C}$. Meanwhile, the increasing importance of UO_2OH^+ at elevated temperatures can be correlated with the decrease in the dielectric constant of water. Such decrease would increase the electrostatic repulsion of the mononuclear “building blocks” and decrease the formation of polynuclear and highly charged species according to simple electrostatic models.³²

In contrast to the hydrolysis constants, only a few data of enthalpy of hydrolysis are available in the literature from 10 to $100 \text{ }^{\circ}\text{C}$ (Figure 4B).^{1–3} The literature values of $\Delta H_{2,2}$ are comparable with the data from this work, but those of $\Delta H_{5,3}$ are much lower. It should be noted that most values of $\Delta H_{n,m}$ in the literature were not directly determined by calorimetry at specific temperatures. Instead, they were obtained by fitting the hydrolysis constants over a temperature range. Besides, the error in the enthalpy of formation of water could significantly affect the accuracy of $\Delta H_{5,3}$, since five water molecules are involved in reaction 6. We believe that the data from this work are more reliable because (1) they were directly determined at variable temperatures by calorimetry; (2) the enthalpy of formation of water in the ionic media was independently determined by calorimetry; and (3) consistent trends were observed over the temperature range from 10 to $85 \text{ }^{\circ}\text{C}$ (Figure 4B).

The hydrolysis reactions 4, 5, and 6 are “isoelectric”, in which the electrostatic contributions to the temperature dependence of the heat capacity of reaction may balance out to a large extent, due to the equality of the same charge between the reactants and products.⁶ As a result, the heat capacity of isoelectric reactions may be small and independent of temperature. Data from this study indicate that $\Delta C_{p(2,2)}$ and $\Delta C_{p(5,3)}$ could indeed be considered constant from 10 to $85 \text{ }^{\circ}\text{C}$, suggested by the linearity of $\Delta H_{2,2}$ and $\Delta H_{5,3}$ in Figure 4B. However, they are not very small: $\Delta C_{p(2,2)}$ and $\Delta C_{p(5,3)}$ are calculated from the slopes in Figure 4B to be 152 ± 43 and $-229 \pm 34 \text{ J K}^{-1} \text{ mol}^{-1}$, respectively.

4.3. Effect of Temperature on the UV/Vis Absorption Spectra. The effect of temperature on the absorption spectra of U(VI) (Figure 3) can be discussed in conjunction with the speciation diagram (Figure 5) and the “deconvoluted” spectra of U(VI) species in the literature.³⁴ The speciation diagram

(32) Plyasunov, A. V.; Grenthe, I. *Geochim. Cosmochim. Acta* **1994**, *58*, 3561–3582.

(33) Grenthe, I.; Spahiu, K.; Plyasunov, A. V. In *Modeling in Aquatic Chemistry*; Grenthe, I., Puigdomenech, I., Eds.; Estimations of Medium Effects on Thermodynamic Data; NEA/OECD: Paris, 1997; Chapter IX.

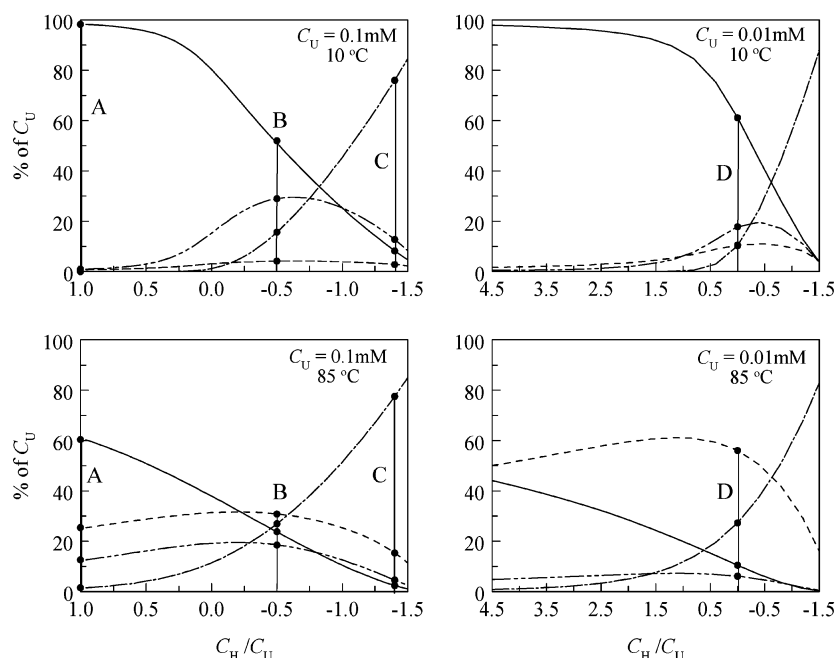


Figure 5. Speciation of U(VI) solutions at 10 °C and 85 °C, $I = 0.10 \text{ mol dm}^{-3}$ ($\text{C}_2\text{H}_5)_4\text{NClO}_4$. (—) UO_2^{2+} , (---) UO_2OH^+ , (-·-·-) $(\text{UO}_2)_2(\text{OH})_2^{2+}$, (····) $(\text{UO}_2)_3(\text{OH})_5^+$. The speciation of U(VI) in solutions A–D is shown as solid symbols.

shows that the extent of hydrolysis increases from solution A to B and to C. Solutions A and C contain mainly the UO_2^{2+} and $(\text{UO}_2)_3(\text{OH})_5^+$, respectively, while solution B contains several U(VI) species in comparable amounts. Previous chemometric and statistical analysis indicates that the maxima of the absorption spectra of UO_2^{2+} , $(\text{UO}_2)_2(\text{OH})_2^{2+}$, and $(\text{UO}_2)_3(\text{OH})_5^+$ are at 414, 421.8, and 429 nm and the molar extinction coefficients are in the order $\text{UO}_2^{2+} < (\text{UO}_2)_2(\text{OH})_2^{2+} < (\text{UO}_2)_3(\text{OH})_5^+$.³⁴ These explain the red shift of the spectra and the increase in absorbance for solutions $\text{A} \rightarrow \text{B} \rightarrow \text{C}$ at each temperature (Figure 3). In fact, the spectra for solution C (Figure 3) are very similar to the spectra for $(\text{UO}_2)_3(\text{OH})_5^+$ in the literature, consistent with the speciation diagram that $(\text{UO}_2)_3(\text{OH})_5^+$ is dominant in solution C (~80%). Furthermore, when the temperature was increased from 10 °C to 85 °C, the further red shift in wavelength and the increase in absorbance for each solution were due to the higher degree of hydrolysis at higher temperatures. This observation is in agreement with the results obtained by thermodynamic measurements.

4.4. Effect of Temperature on the Fluorescence. The speciation of U(VI) indicates that solution C contains mainly $(\text{UO}_2)_3(\text{OH})_5^+$ (~80%) at all the temperatures (Table 2). As a result, the fluorescence properties (the spectra, the lifetime and its dependency on temperature) of solution C represent those of $(\text{UO}_2)_3(\text{OH})_5^+$. As the temperature was increased from 20 to 80 °C, the fluorescence intensity and lifetime of $(\text{UO}_2)_3(\text{OH})_5^+$ decreased, but the emission spectrum remained almost unchanged. Based on the electron–phonon coupling model on the basis of Franck–Condon transition,³⁵ the O=U=O stretching frequency in $(\text{UO}_2)_3(\text{OH})_5^+$ was calculated to be approximately 750 cm^{-1} . This value is quite low in comparison with those of U(VI) in solids and aqueous solutions of low pH (usually $> 800 \text{ cm}^{-1}$)³⁶ and much lower than the symmetrical stretching vibration frequencies of hydrolyzed U(VI) species

in solution observed by Raman spectroscopy: $848 \pm 2 \text{ cm}^{-1}$ for $\text{UO}_2(\text{OH})^+$, $854 \pm 2 \text{ cm}^{-1}$ for $(\text{UO}_2)_2(\text{OH})_2^{2+}$, and $835 \pm 1 \text{ cm}^{-1}$ for $(\text{UO}_2)_3(\text{OH})_5^+$.^{38–40} It is known that the strong bonding of equatorial ligands such as OH^- could weaken and lengthen the O=U=O bonds, but the exact nature of the electronic structure and bonding in the uranyl complexes is still unclear.³⁷ Further investigations are needed to understand the mechanisms that lead to the significant changes of the vibrational frequency in hydrolyzed U(VI) species.

As Table 2 indicates, the lifetimes and activation parameters for $(\text{UO}_2)_3(\text{OH})_5^+$ from this study agree with some data in the literature but differ from others.^{25–27} Due to the absence of experimental details on data collection and processing in previous studies, the reason for the difference remains unclear.

Solution B contains all four species in comparable amounts (Table 2). Consequently, the fluorescence properties could reflect the overall effect of all the species or, more probably, depend on the species that has the highest absorption coefficient and/or the highest fluorescence yield. $(\text{UO}_2)_3(\text{OH})_5^+$ is likely to be such a species, since its molar absorption coefficient at 430 nm is much higher than the other species.³⁴ As a result, the fluorescence lifetime and activation parameters for solution B were very similar to but slightly lower than those of solution C where $(\text{UO}_2)_3(\text{OH})_5^+$ was dominant.

4.5. Test of Approximation Approaches. Values of $\log * \beta_{2,2}^{\circ}$ and $\log * \beta_{5,3}^{\circ}$ from 10 to 85 °C were calculated with the approximation approaches previously mentioned except the revised HFK equation. The latter approach was not tested due to the lack of parameters for polynuclear U(VI) species.

(36) Bartlett, J. R.; Cooney, R. J. *Mol. Struct.* **1989**, *193*, 295–300.

(37) Clark, D. L.; Conradson, S. D.; Donohoe, R. J.; Keogh, D. W.; Morris, D. E.; Palmer, P. D.; Rogers, R. D.; Tait, C. D. *Inorg. Chem.* **1999**, *38*, 1456–1466.

(38) Quiles, F.; Burneau, A. *Vib. Spectrosc.* **1998**, *18*, 61–75.

(39) Nguyen-Trung, C.; Palmer, D. A.; Begun, G. M.; Peiffert, C.; Mesmer, R. E. *J. Solution Chem.* **2000**, *29*, 101–129.

(40) Fujii, T.; Fujiwara, K.; Yamana, H.; Moriyama, H. *J. Alloys Compd.* **2001**, *323–324*, 859–863.

(34) Meinrath, G. *Radiochim. Acta* **1997**, *77*, 221–234.

(35) Liu, G. K.; Chen, X. Y.; Huang, J. *Mol. Phys.* **2003**, *101*, 1029.

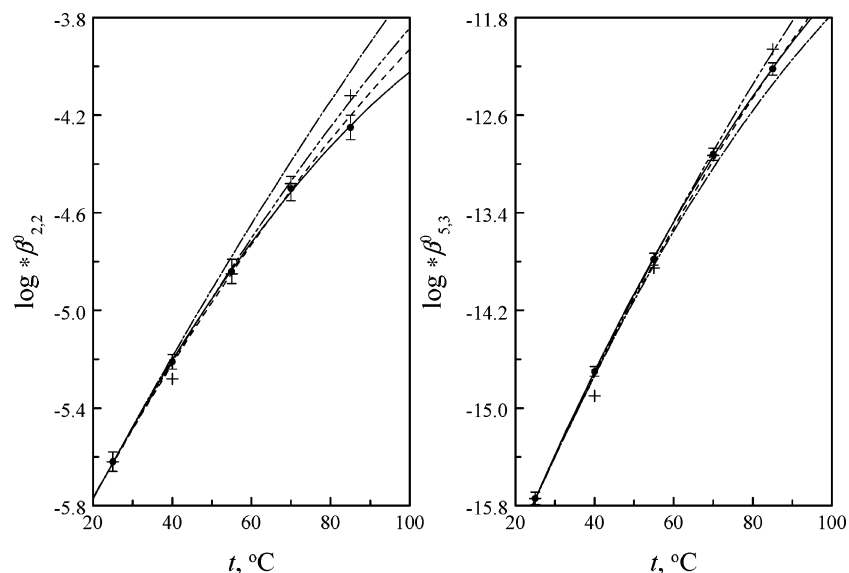


Figure 6. Test of three approximation approaches for prediction of temperature effect on the hydrolysis of U(VI), $I = 0.10 \text{ mol dm}^{-3} (\text{C}_2\text{H}_5)_4\text{NClO}_4$. (—•—) experimental data from this study, (---) constant enthalpy of hydrolysis, (-·-) constant heat capacity of hydrolysis, (····) DQUANT equation, (+) Ryzhenko–Bryzgalin model.

Calculations with the constant enthalpy approach, the constant heat capacity approach, and the DQUANT equation are straightforward, and the parameters used in the calculation are from this work, including $\Delta H_{n,m(298)}$, $\Delta S_{n,m(298)}$, and $\Delta C_{p(n,m)}$.

The Ryzhenko and Bryzgalin model,⁸ based on simple electrostatic theories, describes the temperature dependence of the formation of a mononuclear complex ($M^{m+} + jL^{n-} = ML_j^{(m-nj)+}$). It has been extended to analyze the polynuclear U(VI) hydroxide complexes.³² To use this model, the entropies of hydrolysis for reactions 5 and 6 were converted to the entropies of complexation for reactions 10 and 11:



by using the standard entropy of water formation.¹ From the entropy of complexation, a parameter $R1$ (a function of the effective charge ($|Z_M Z_L|$) and coordination geometry) and an effective bond distance (r_{eff}) were estimated. The formation constants of polynuclear U(VI) hydroxide complexes at other temperatures were calculated by

$$\log K_T^\circ = \log K_{298}^\circ(298.15/T) + (R1/r_{\text{eff}}) \times e^2 N(1/\epsilon_T - 1/\epsilon_{298}) / (RT \ln 10) \quad (12)$$

where K_T° and K_{298}° are the formation constants at T and 298.15 K, $e^2 N = 13.895 \times 10^5 \text{ J mol}^{-1}$, and ϵ_T and ϵ_{298} are the dielectric constants of water at T and 298.15 K.³²

The entropies of complexation for $(\text{UO}_2)_2(\text{OH})_2^{2+}$ and $(\text{UO}_2)_3(\text{OH})_5^+$ at 25 °C were calculated to be $216 \pm 6 \text{ J K}^{-1} \text{ mol}^{-1}$

and $506 \pm 7 \text{ J K}^{-1} \text{ mol}^{-1}$. From these, the values of $(R1/r_{\text{eff}})$ were estimated to be 2.68 and 6.27 for $(\text{UO}_2)_2(\text{OH})_2^{2+}$ and $(\text{UO}_2)_3(\text{OH})_5^+$. The formation constants were accordingly calculated with eq 12 and converted back to the hydrolysis constants for reactions 5 and 6.

The calculated values of $\log * \beta_{2,2}^\circ$ and $\log * \beta_{5,3}^\circ$ are compared with the experimental data in Figure 6. All four approaches provide quite satisfactory predictions of the hydrolysis constants at temperatures up to 60–70 °C. Deviations start to increase as the temperature is increased, reaching 0.1 logarithm unit (~ 2 times larger than the 3σ of the experimental data) at 70–80 °C for both $\log * \beta_{2,2}^\circ$ and $\log * \beta_{5,3}^\circ$. The constant enthalpy approach provides the best prediction for $\log * \beta_{5,3}^\circ$, with deviations within the uncertainty of the data at temperatures up to 85 °C.

Acknowledgment. This work was supported by the Director, Office of Science, Office of Basic Energy Sciences, Division of Chemical Sciences, under U.S. Department of Energy Contract No. DE-AC03-76SF0098 at the Lawrence Berkeley National Laboratory Contract No. W-31-109-ENG-38 at Argonne National Laboratory, and by the Ministero dell'Università e della Ricerca Scientifica e Tecnologica (MURST, Roma) within the program COFIN02.

Supporting Information Available: Experimental conditions of potentiometry and calorimetry and potentiometric titration and fluorescence spectra data (three tables and four figures). This material is available free of charge via the Internet at <http://pubs.acs.org>.

JA0398666